MODELING OF MAGNETOSTATIC SURFACE OSCILLATIONS IN ELLIPTIC NANOTUBES

M.A. POPOV, I.V. ZAVISLYAK

Taras Shevchenko Kyiv National University
(64, Volodymyrs'ka Str., Kyiv 01033, Ukraine; e-mail: zav@univ.kiev.ua)

UDC 537.876

The theory of magnetostatic surface oscillations (MSSOs) in a ferromagnetic tube with elliptic cross-section is presented. Resonance frequencies and magnetic field lines are calculated. It is found that the spectrum of elliptic oscillations of a tube consists of two families (low and high frequencies), and the energies of oscillations of those families tend to localize on the outer and inner surfaces of the tube. The theoretical results are compared with experimental data on the spectra of three-layer nanostructures, and a satisfactory agreement is achieved.

1. Introduction

Progress achieved in lithographic techniques allows the fabrication of high-quality well-controlled magnetic structures like dots, wires, and multilayered structures of micron- or nanosizes. Although the static properties of such entities have been studied to some extent, their high-frequency dynamic properties are the subject of up-to-date investigations. The study of spin waves and oscillations is a powerful method of probing the dynamic properties of magnetic media in general and laterally patterned structures in particular. In nanoobjects, the quantization effects lead to significant changes in the spin wave spectrum, especially for objects of complicated shape.

The simplest two-dimensional magnetic structures for modeling are nanowires which can be regarded as infinitely long cylinders of elliptic cross-section. Magnetostatic surface modes in an axially magnetized elliptic cylinder in the nonexchange approximation were first considered in [1], where the Walker's equation [2] was solved in the standard elliptic cylindrical coordinates.

MSSOs in elliptic cavities and cylinders were discussed in [3]. The solution of the problem of eigenmodes for an elliptic tube was given in [4]. In these papers, an original analytical approach to the solution of such problems, based on modified elliptic cylindrical coordinates, was developed.

This method supplements the previously reported ones [5–8] and allows one to examine the two-dimensional spectral problems for magnetic structures with the elliptic geometry of cross-sections in the analytical convenient fashion.

The objective of this study is to investigate MSSOs in elliptic tubes theoretically, to analyze spectra and fields of eigenmodes, and to compare the obtained results with the experimental data.

2. Theory of MSSOs in a Ferromagnetic Tube of Elliptic Cross-Section

2.1. General solution. Eigenfrequency spectrum

We use an approach based on the direct solution of Maxwell's equations in the magnetostatic approximation. It is justified by the fact that the employment of a magnetostatic potential for this and similar problems leads to a rather sophisticated characteristic equation sometimes containing spurious expressions need to be excluded. It is determined by the complex dependence of permeability tensor components on the mode frequency. This problem will be more severe when the geometry of a sample becomes more complicated.

Let us consider an infinitely long ferromagnetic tube with elliptic cross-section subjected to an external static magnetic field $\vec{H}_0$ applied along the tube axis which coincides with the z-axis of our coordinate system (Fig. 1).

We use the nonexchange magnetostatic approximation. The maximum value of the wave vector, when the exchange can be still neglected, is defined by the condition [9]

$$k_{\max} = \sqrt{\Delta H/D},$$

where ΔH is the spin-wave line width, and D is the exchange stiffness. For metallic ferromagnets, one can take typical value ΔH=50 Oe and $D = 2.5 \times 10^9 \mathrm{Oe{\cdot}cm^2}$ and calculate $k_{\max} = 14 \times 10^4 \mathrm{cm^{-1}}$. For an elliptic tube, the following formula for the quantized wave number

follows from geometric considerations:

$k_m = m/a,$

where $a = a_1, a_2$, and m is a positive integer.

If we consider the typical experimental major semiaxis of the order of magnitude of 1 μm, we obtain $k_m = m \times 10^4$ cm^{-1}. Hence, when we examine oscillations with $m < 10$, the exchange interaction can be omitted without any perceptible mistake.

In thin ferromagnetic films subjected to an in-plane magnetic field, standing spin wave resonances can occur with eigenfrequencies given by [9]

$$\omega_n^2 = \left(\omega_H + \gamma D k_n^2\right)\left(\omega_H + \gamma D k_n^2 + \omega_M\right),$$

where $k_n = n\pi/s$, and s is the thickness of a film.

In our case, $s \approx b_2 - b_1$. Calculations made by this formula have proved that, in all experiments mentioned below, the lower standing spin wave resonance (with $n = 1$) frequency is higher than observed magnetostatic resonance frequencies. Thus, there is a wide frequency range, where it is possible to analyze magnetic oscillations in the nonexchange magnetostatic approximation.

We start from the pair of Maxwell's equations in the magnetostatic approximation for complex-phasor space vectors of the magnetic field and the magnetic induction, by assuming the time dependence as $e^{j\omega t}$:

$$\mathrm{rot}\vec{H} = 0, \quad \mathrm{div}\vec{B} = 0. \tag{1}$$

To solve these equations, we used modified elliptic cylindrical coordinates defined by the relations

$$x = (\rho + \frac{c^2}{4\rho})\cos\varphi \quad , \quad y = (\rho - \frac{c^2}{4\rho})\sin\varphi,$$

$$\varphi \in [-\pi, \pi], \quad \rho \in [\frac{c}{2}, \infty),$$

where c is the semifocal length, $c = \sqrt{a_1^2 - b_1^2} = \sqrt{a_2^2 - b_2^2}$, and a_i and b_i are the semimajor and semiminor axes, respectively. This substitution is a modification of the standard elliptic cylindrical coordinates used in [1]. It is more useful, because it provides a convenient transition to the circular case and polar coordinates (when $c = 0$). In addition, it allows one to avoid a non-physical divergence in the foci of the ellipse and to analyze analytically a magnetic field, on the contrary to [10].

The metrical coefficients (Lamé scale factors) are

$$h_\rho = \sqrt{\left(1 - \frac{c^2}{4\rho^2}\right)^2 + \frac{c^2}{\rho^2}\sin^2\varphi} \quad , \quad h_\varphi = \rho h_\rho.$$

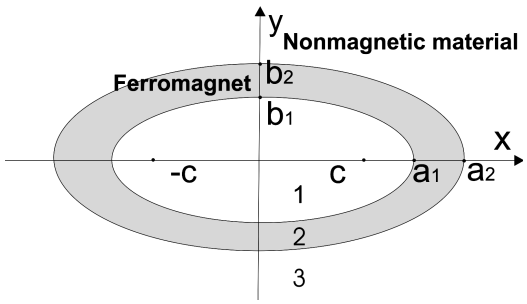

Fig. 1. Geometry of an elliptic tube: *1* and *3* – nonmagnetic material, and *2* – ferromagnet

In this coordinate system, an ellipse with semiaxes a_i and b_i is defined by the relation $\rho = R_i = \mathrm{const}$, where $R_i = \frac{a_i + b_i}{2}$, i=1,2.

We describe a material by the tensor nonsusceptibility $\widehat{\eta}$ defined by the relation

$$\vec{H} = \widehat{\eta}\vec{M}, \tag{2}$$

where $\widehat{\eta} = \begin{pmatrix} \eta & -i\eta_a \\ i\eta_a & \eta \end{pmatrix}$, $\eta_a = \frac{4\pi\omega}{\omega_M}$, $\eta = \frac{4\pi\omega_H}{\omega_M}$, $\omega_M = \gamma 4\pi M$, $\omega_H = \gamma H_0$, γ is the gyromagnetic ratio, and $M$is the saturation magnetization.

We will use the results presented in [4]. According to them, we have

$$H_\rho^{(1)}(\rho,\varphi) = \frac{1}{h_\rho \rho^{n+1}}\Big(E(\rho^{2n} - (c/2)^{2n})\cos(n\varphi) + F(\rho^{2n} + (c/2)^{2n})\sin(n\varphi)\Big),$$
$$H_\varphi^{(1)}(\rho,\varphi) = \frac{1}{h_\rho \rho^{n+1}}\Big(F(\rho^{2n} - (c/2)^{2n})\cos(n\varphi) - E(\rho^{2n} + (c/2)^{2n})\sin(n\varphi)\Big)$$

in region 1,

$$M_\rho(\rho,\varphi) = \frac{1}{h_\rho \rho}\left((A\rho^n + B\rho^{-n})\cos(n\varphi) + (C\rho^n + D\rho^{-n})\sin(n\varphi)\right),$$
$$M_\varphi(\rho,\varphi) = \frac{1}{h_\rho \rho}\left((C\rho^n - D\rho^{-n})\cos(n\varphi) + (-A\rho^n + B\rho^{-n})\sin(n\varphi)\right)$$

in region 2, and

$$H_\rho^{(3)}(\rho,\varphi) = \frac{1}{h_\rho \rho^{n+1}}\left(G\cos(n\varphi) + K\sin(n\varphi)\right),$$
$$H_\varphi^{(3)}(\rho,\varphi) = \frac{1}{h_\rho \rho^{n+1}}\left(-K\cos(n\varphi) + G\sin(n\varphi)\right)$$

in region 3.

The magnetic field components inside the ferromagnetic can be expressed by using (2). The dispersion equation has the form

$$(1+P)^2\omega^4 - s\omega^2 + q = 0, \tag{3}$$

where

$$s = (1/4\omega_M^2(1-r^{4n})(1-P)^2+$$

$$+2\omega_H(1+P)^2(\omega_M+\omega_H) + 2\omega_M^2 P(1-r^{2n})),$$

$$q = (\omega_H^2(1+P) + 1/2\omega_M^2(1-r^{2n})+$$

$$+1/2\omega_M\omega_H(r^{2n}(P-1) + (P+3)))\times$$

$$\times(\omega_H^2(1+P) + 1/2\omega_M^2 P(1-r^{2n})+$$

$$+1/2\omega_M\omega_H(r^{2n}(1-P) + (3P+1))),$$

$$P = (1-(c/2R_1)^{2n})/(1+(c/2R_1)^{2n}),$$

$$r = R_1/R_2, \quad R_1 = \frac{a_1+b_1}{2}, \quad R_2 = \frac{a_2+b_2}{2}.$$

This equation is biquadratic, and it roots can be expressed as

$$\omega_n^+ = \frac{1}{(1+P)}\sqrt{1/2\,(s+\sqrt{s^2-4(1+P)^2q})}, \tag{4}$$

$$\omega_n^- = \frac{1}{(1+P)}\sqrt{1/2\,(s-\sqrt{s^2-4(1+P)^2q})}, \quad n>0. \tag{5}$$

Thus, the solution manifests two frequency families. The frequency of azimuthally independent oscillations can be obtained formally from (4), if we substitute $n=0$. In the frames of the current theory (an infinitely long sample, the non-exchange approximation), the radial bulk modes [11] are absent.

2.2. Magnetic field lines

In our curvilinear 2-dimensional coordinate system, the differential equation describing the field lines has the form [12]

$$\frac{h_\rho d\rho}{\mathrm{Re}\{H_\rho\cdot e^{j\omega t}\}} = \frac{h_\varphi d\varphi}{\mathrm{Re}\{H_\varphi\cdot e^{j\omega t}\}}. \tag{6}$$

By substituting the expressions for magnetic fields in a proper region into (6) and integrating the left-hand and right-hand sides, we obtain

$$\left(\rho^n - \left(\frac{c^2}{4\rho}\right)^n\right)\sin(n\varphi)\cos(\omega t)+$$

$$+M_1\left(\rho^n + \left(\frac{c^2}{4\rho}\right)^n\right)\cos(n\varphi)\sin(\omega t) = \mathrm{const} \tag{7}$$

for region 1, where

$$M_1 = -\frac{1}{P}\frac{\eta - i\frac{A}{C}\eta_a - (\eta\frac{D}{C} + i\frac{B}{C}\eta_a)R_1^{-2n}}{\eta_a - i\frac{A}{C}\eta + (\frac{D}{C}\eta_a + i\eta\frac{B}{C})R_1^{-2n}},$$

$$((\eta_a - i\frac{A}{C}\eta)\rho^n - (\frac{D}{C}\eta_a + i\frac{B}{C}\eta)\rho^{-n})\sin(n\varphi)\cos(\omega t)-$$

$$-((\eta - i\frac{A}{C}\eta_a)\rho^n + (\frac{D}{C}\eta + i\frac{B}{C}\eta_a)\rho^{-n})\times$$

$$\times\cos(n\varphi)\sin(\omega t) = \mathrm{const} \tag{8}$$

for region 2, and

$$\frac{\sin(n\varphi)\cos(\omega t) + M_2\cos(n\varphi)\sin(\omega t)}{\rho^n} = \mathrm{const} \tag{9}$$

for region 3, where

$$M_2 = -\frac{\eta - i\frac{A}{C}\eta_a - (\eta\frac{D}{C} + i\frac{B}{C}\eta_a)R_2^{-2n}}{\eta_a - i\frac{A}{C}\eta + (\frac{D}{C}\eta_a + i\eta\frac{B}{C})R_2^{-2n}}.$$

Expressions like A/C can be found from the set of equations for boundary conditions together with (3). They depend on magnetic and geometric parameters of the structure only.

2.3. Energy distribution and ellipticity

To analyze the energy distribution of oscillations in a ferrite tube, we have calculated the circumferential component of the Poynting vector $P_\varphi = \frac{c}{8\pi}\mathrm{Re}(H_\rho^* E_z)$. The electric field component E_z can be found in the first approximation from another pair of Maxwell's equations [9].

The normalized circumferential components of the Poynting vector $P_\varphi(\rho, \varphi = \pi/4)$ of oscillations with $n = 1, 3, 5$ for both low-frequency and high-frequency families are depicted in Fig. 2 with a reduced variable $(\rho - R_1)/(R_2 - R_1)$ along the abscissa. For other values of φ, the picture will be qualitatively the same. One can

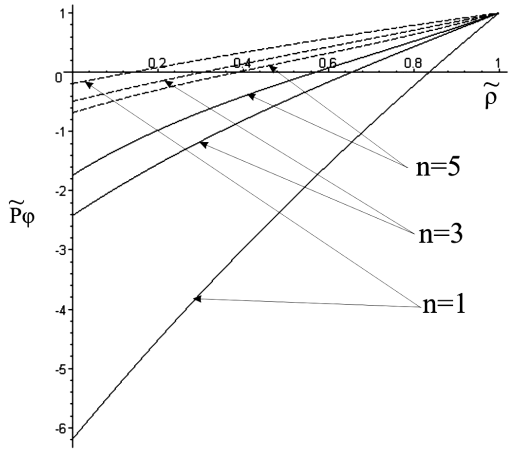

Fig. 2. Radial distribution of the energy in an elliptic ferromagnet tube, $\widetilde{P}_\varphi = \frac{P_\varphi(\rho,\varphi=\pi/4)}{P_\varphi(R_2,\varphi=\pi/4)}$, $\widetilde{\rho} = (\rho - R_1)/(R_2 - R_1)$. Here, n=1, 3, 5 is the mode number; solid lines – the low-frequency family, dashed lines – the high-frequency family

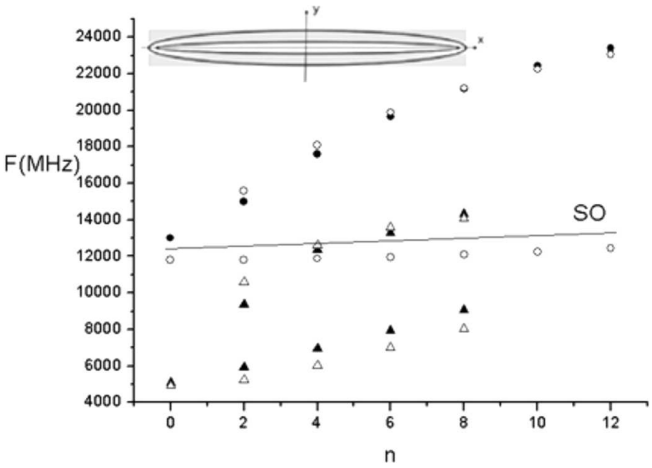

Fig. 3. MSSOs frequencies versus the mode number n in the $Ni_{81}Fe_{19}$(30 nm)/Cu(10 nm)/ $Ni_{81}Fe_{19}$(30 nm) structure (triangles) and in Fe(20 nm)/Au(3 nm)/Fe(20 nm) (circles). Open symbols – theory, solid symbols and the line – experiment

see that the energy tends to localize on the surfaces (outer and inner) of the tube. The absolute value of the Poynting vector is greater on the inner surface for the low-frequency families and on the outer surface for the high-frequency ones.

In addition, the circumferential direction of energy circulation is opposite on the different surfaces: it is clockwise on the inner surface and counterclockwise on the outer one for both families. Thus, we have two energy fluxes: one of them is concentrated primarily on the inner surface and rotates clockwise, and the other is concentrated on the outer surface and rotates counterclockwise.

Another interesting theoretical result is the following: the ellipticity of the high-frequency magnetization (defined as $\varepsilon = 1 - (m_{\min}/m_{\max})^2$, where $m_{\min}$ and $m_{\max}$ are the semiminor and semimajor axes of the polarization ellipse, according to [9]) of both families is uniform throughout the tube's cross-section (except for the points with $\rho = (D/C)^{-1/(2n)} = (-B/A)^{-1/(2n)}$, $\varphi = m\pi/n$, $m = 0, 1, 2..$ or $\rho = (-D/C)^{-1/(2n)} = (B/A)^{-1/(2n)}$, $\varphi = (m + 1/2)\pi/n$, $m = 0, 1, 2..$, where M_ρ and M_φ are both equal to zero, and thus the polarization is uncertain). The ellipticity of the magnetization precession has the following peculiarities: 1) the ellipticity decreases when the oscillation's number increase and, hence, the polarization tends to be circular; 2) the ellipticity of the high-frequency family is lower than that of the low-frequency family; 3) for oscillations with low numbers, the ellipticities of the high- and low-frequency families differ noticeably, while they are almost equal for oscillations with large numbers.

3. Application of the Theory of MSSOs to Brillouin Light Scattering Spectra of Three-Layer Structures

We have failed to find out any experiments on the magnetostatic resonance in elliptic ferromagnetic nanotubes; however, there are some investigations of MSSOs in three-layer ferromagnet-nonmagnetic spacer-ferromagnet nanostructures [7, 8]. In those structures, the inequalities $l \gg d \gg s$ are satisfied, where l is the length, d is the width, and s is the thickness of a nanostructure, which allows us to approximate it with an infinitely long elliptic tube (see the inset in Fig. 3). This enables the interpretation of the experimental MSSOs spectra according to the stated theory.

In [7], spin-wave excitations in long threelayer nanostructures of the composition $Ni_{81}Fe_{19}$(30 nm)/ Cu(10 nm)/$Ni_{81}Fe_{19}$(30 nm) with rectangular cross-section were investigated. The measured frequencies of nonexchange magnetostatic oscillations from [7] (solid triangles) are compared with ones calculated using (4) and (5) (open triangles) in Fig. 3.

As can be seen from Fig. 3, the theoretical and experimental dependences match qualitatively and, to a great extent, quantitatively. The important thing is that the theoretical prediction about two families of oscillations is approved experimentally. As for the

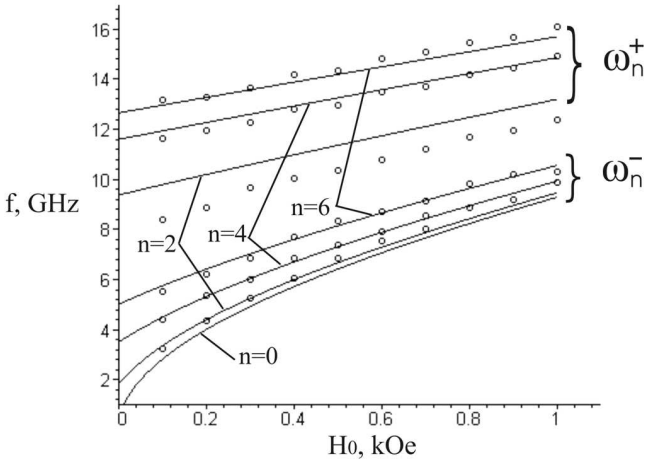

Fig. 4. MSSOs frequencies versus the magnetic field intensity for the $Ni_{81}Fe_{19}$(30 nm)/Cu(10 nm)/ $Ni_{81}Fe_{19}$(30 nm) three-layer structure

quantitative comparison, for the high-frequency family, theory and experiment match with the only one exception (n=2); and, for the low-frequency family, the discrepancy is less than 12%, which is resulted, possibly, from the imperfect data on magnetic and geometric parameters of the sample.

The other output from [7] is the dependence of the frequency of spin wave oscillations on a magnetic field. It is depicted in Fig. 4 together with the theoretical results obtained from (4) and (5). One can see that the coincidence is rather good except for high-frequency oscillations with n=2, where the error is as large as 14 %. Note that, in the n=0 case, the high- and low-frequency families are degenerated.

In [8], spin-wave excitations in long three-layer nanostructures of the composition Fe(20 nm)/Au(3 nm)/ Fe(20 nm) were investigated. The MSSOs frequencies calculated with the use of the presented theory (open circles) and the experimental data (solid circles and line) are presented in Fig. 3. The authors obtained a low-frequency family and treated it as a surface optic mode (SO), but they weren't able to distinguish separate modes experimentally.

Once again, we observe the good coincidence of the high-frequency family and a mismatch of about 10 % for the low-frequency or SO family.

In summary, we can state that the developed theory describe MSSOs in three-layer structures rather well. The discrepancies can be explained by the following reasons: more pronounced differences between a real sample and the elliptic tube model for three-layer structures; insufficient accuracy of BLS measurements; absence of the exhaustive information about experimental conditions.

4. Conclusions

A theory of surface magnetostatic oscillations in ferromagnetic tubes of elliptic cross-section has been developed. On the basis of this theory, the MSSO resonance frequencies are determined as the functions of the saturation magnetization, the external field, and the geometric parameters of the tube. The formulas describing the magnetic field lines have been obtained.

It is shown that the MSSO spectrum contains two families – low- and high-frequency ones. The energies of oscillations for these families tend to localize on the surfaces (outer and inner) of the tube. The absolute value of the Poynting vector is greater on the inner surface for oscillations of the low-frequency family and on the outer surface for oscillations of the high-frequency one.

The suggested theory is applied to the interpretation of the experimental data obtained by the BLS technique on layered nanostructures. A good agreement between the theory and the experiment demonstrates that this theory is applicable to calculations of the spectrum of three-layer nanostructures.

1. R.E. De Wames and T. Wolfram, Appl. Phys. Lett. **16,** 8 (1970).
2. L.R. Walker, Phys. Rev. **105**, 2 (1957).
3. I.V. Zavislyak, G.P. Golovach, M.A. Popov, and V.F. Romanyuk, J. Commun. Tech. and Electron. **51**, 2 (2006).
4. M.A. Popov and I.V. Zavislyak. Radio Elect. and Commun. Systems **49**, 6 (2006).
5. R. Arias and D.L. Mills, Phys. Rev. B **63**, 13 (2001).
6. R. Arias and D.L. Mills, Phys. Rev. B **70**, 9 (2004).
7. G. Gubbiotti, M. Kostylev, N. Sergeeva *et al.*, Phys. Rev. B **70**, 22 (2004).
8. N. Sergeeva, S.-M. Cherif, A. Stachkevitch *et al.*, Phys. Status Solidi C **1**, 7 (2004).
9. A.G. Gurevich and G.A. Melkov, *Magnetization Oscillations and Waves* (CRC Press, New York, 1996).
10. Y. Roussigne and P. Moch, J. Phys. Condens. Matter. **17**, 10 (2005).
11. I. Joseph and E. Schlomann, J. Appl. Phys. **32**, 6 (1961).
12. A.D. Grigor'ev, *Electrodynamics and Technique of SHF* (Vysshaya Shkola, Moscow, 1990) (in Russian).

Received 01.11.07

МОДЕЛЮВАННЯ ПОВЕРХНЕВИХ
МАГНІТОСТАТИЧНИХ КОЛИВАНЬ
В ЕЛІПТИЧНИХ НАНОТРУБКАХ

М.О Попов, І.В. Зависляк

Р е з ю м е

Представлена теорія поверхневих магнітостатичних коливань в феромагнітних трубках еліптичного перерізу. Знайдено резонансні частоти та вирази для силових ліній магнітного поля. Показано, що спектр коливань складається з двох груп – високочастотної та низькочастотної, – енергія яких локалізована переважно на поверхнях (внутрішній і зовнішній) трубки. Показано можливість застосування даної теорії для інтерпретації спектрів тришарових наноструктур, отримано непогане узгодження теоретичних результатів з експериментальними.